Sparsely synchronized neuronal oscillations

Nicolas Brunel[a)]
Laboratoire de Neurophysique et Physiologie, Université Paris Descartes, 45 rue des Saints Pères, 75270 Paris Cedex 06, France and UMR 8119, CNRS, 45 rue des Saints Pères, 75270 Paris Cedex 06, France

Vincent Hakim[b)]
Laboratoire de Physique Statistique, CNRS-UMR8550, Associé aux Universités Paris VI et VII, Ecole Normale Supérieure, 24 rue Lhomond, 75231 Paris Cedex 05, France

(Received 6 February 2007; accepted 26 July 2007; published online 27 March 2008)

We discuss here the properties of fast global oscillations that emerge in networks of neurons firing irregularly at a low rate. We first provide a simple introduction to these sparsely synchronized oscillations, then show how they can be studied analytically in the simple setting of rate models and leaky integrate-and-fire neurons, and finally describe how various neurophysiological features can be incorporated in this framework. We end by a comparison of experimental data and theoretical results. © *2008 American Institute of Physics*. [DOI: 10.1063/1.2779858]

Electrical recordings of brain activity show a diversity of neural rhythms that can be correlated with stages of sleep and with tasks during wakefulness. These neural oscillations reflect the synchronized discharge of a large number of neurons. They were first studied by assimilating neurons to nonlinear oscillators that emitted action potentials in a periodic fashion. However, this classic Huygens mode of synchronization is fragile and, in several instances, seems at odds with available experimental data on the discharge patterns of individual cells. Here, we explain and discuss work performed in the past few years on a different mode of synchronization in which a fast collective oscillation is produced by neurons firing in a stochastic way and at a low rate compared to the oscillation period.

I. INTRODUCTION

Oscillations have been known to be a prominent feature of neural activity since Hans Berger published the EEG of his son[1] and Lord Adrian confirmed their presence in different brain structures[2] such as the olfactory bulb and the cerebellum. In recent years, a number of experimental and theoretical works have been devoted to try and better understand the mechanisms underlying these neural rhythms that appear in a large range of frequency bands from very slow (<1 Hz) to very high frequencies (≥ 200 Hz), and are structure- and task-specific. It has in particular become apparent that in many instances inhibition is playing an important role in synchronizing neural firing. This has first been shown theoretically for an oscillation mode in which neurons fire synchronously and in a regular fashion at a rate close to the frequency of the network oscillation.[3,4] In this regime, neurons behave similarly to nonlinear oscillators and their synchronization can be described using standard techniques.[5]

This synchronous oscillation mode is, however, easily disrupted by noise and heterogeneity. Moreover, single neurons *in vivo* typically fire at rates that are much lower than the frequency of the fast oscillations recorded in local field potentials. It was therefore proposed and shown in a simplified model[6] that recurrent inhibition allows a network to generate a distinct and more robust type of oscillation in which a fast rhythm at the network level emerges from sparsely synchronized neurons discharging at a lower frequency. Figure 1 is an example of a network simulation in this regime. Subsequent investigations[7–11] have considered more realistic models that allow for quantitative comparisons with experimental results.

The goal of the present paper is to introduce and briefly survey this body of work. In the first section, we describe oscillations in a population of neurons coupled by inhibition using a rate formalism. This simple description, although approximate, makes it clear that the network oscillation frequency and the cell discharge are independent quantities. In Sec. II, we explain how a quantitative description of sparsely synchronized oscillations can be obtained for networks of inhibitory leaky-integrate-and-fire (LIF) neurons.[6] We then show how the introduced formalism allows for the inclusion of more realistic descriptions of the post-synaptic current[9] (i.e., inclusion of a rise and decay time) and of the single neuron dynamics (i.e., stimulation by correlated noise,[12,13] finite rise time of the action potential,[14] subthreshold resonance,[15,16] etc.). Section III describes the crossover with increasing noise from the classical regime of fully synchronized oscillations to the sparsely synchronized regime.[11] The sparsely synchronized oscillations in mixed networks of excitatory and inhibitory neurons[7,9] are dealt with in Sec. IV. Finally, Sec. V is devoted to comparisons between theoretical results and experimental data.

In the context of this focus issue on mixed-mode oscillations (MMOs), it seems worth noting that dynamics with two frequency scales can emerge in neural systems in many qualitatively different ways. First, the dynamics of isolated

[a)]Electronic mail: nicolas.brunel@univ-paris5.fr.
[b)]Electronic mail: vincent.hakim@ens.fr.

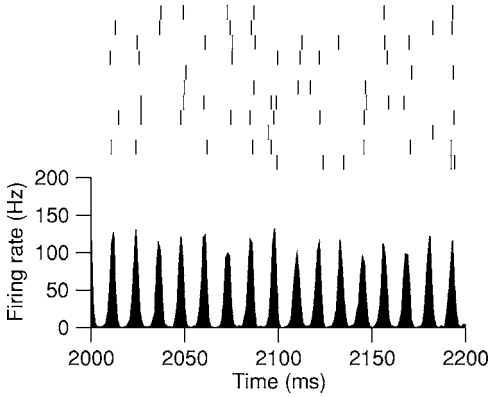

FIG. 1. Oscillations with sparsely firing neurons in a fully connected network of 1000 leaky integrate-and-fire neurons receiving independent white noise sources. The top panel shows a raster of 10 neurons, while the bottom panel shows the network instantaneous firing rate (computed in 1 ms bins). The network oscillates at about 90 Hz, while single cells fire at about 30 Hz, as predicted by the theory—at such frequencies, the neuronal phase lag is close to its high-frequency limit of 45 degrees, while the synaptic phase lag computed from Eq. (32) gives 135 degrees (synaptic time constants: 1 ms latency, 1 ms rise time, 6 ms decay time).

single cells can show two frequencies, the cell spiking rate and one additional frequency coming from intrinsic subthreshold membrane characteristics. The latter can give rise to a subthreshold oscillation[17,18] or simply a resonance in the subthreshold dynamics.[15] Second, the network dynamics itself can create a frequency that is different from the cells spiking rate, as e.g., in fast 200 Hz oscillations seen in the local field potential in the hippocampus, while single cells spike at much lower rates (8–30 Hz).[19] This is the phenomenon on which we concentrate in this short survey. A third possibility that we do not consider here is the coexistence in the global network dynamics itself of two frequencies, a case in point being the mixed theta-gamma oscillations in the hippocampus.[20]

In the scenario on which we focus here, the voltage dynamics of a single neuron presents two well-separated frequency scales, a fast subthreshold frequency imposed by the collective network oscillation, together with the much lower firing frequency of the neuron. As will be discussed later, the firing process itself can be strongly irregular, as in the example of Fig. 1, or almost periodic for small noise levels [see Fig. 6(b)], the case that most resembles standard MMOs.

II. OSCILLATIONS IN RATE MODELS

A classic approach to characterize the dynamics of a large neural network consists in writing a dynamical equation for its instantaneous discharge rate[21] (i.e., the total number of spikes emitted in a small time bin). Such models are sometimes referred to as "rate models" or "neural field models." We start by following this heuristic procedure to investigate the occurrence of oscillations in a network of neurons coupled by inhibition. This has the merit of simplicity and provides useful qualitative insights that can be put on firmer grounds by more complicated computations, as described in the following sections. Here, the discharge rate $r(t)$ of the network is assumed to obey the following equation:

$$\tau \frac{dr}{dt} = -r + \Phi[I_{\text{ext}} - Jr(t-D)], \tag{1}$$

where $\Phi(I)$ is the mean discharge rate of a cell in the network when it receives the current I. In the neuroscience literature, the function $\Phi(I)$, which gives the neuron discharge frequency for a given applied current I, is commonly called the neuron f-I curve. In Eq. (1) the mean inhibitory synaptic current entering neurons in the network at time t, $Jr(t-D)$, is simply supposed to be proportional, with a weight J, to the network activity at time $t-D$, where the delay D accounts in an effective way for the latency and the finite kinetics of the synaptic currents (see Sec. III B for a more detailed description). In a steady situation, the mean firing rate r_0 is given by the fixed point of the dynamics,

$$r_0 = \Phi(I_{\text{ext}} - Jr_0). \tag{2}$$

One can then follow a standard procedure (see, e.g., Ref. 22) to examine the stability of this fixed point. We linearize Eq. (1) and consider small departures $r(t)$ from r_0 in the form $r(t)=r_0+\text{Re}[\hat{r}_1 \exp(\lambda t)]$, where Re denotes "real part." The linear stability spectrum is thus determined by the eigenvalues λ that obey

$$\tau\lambda = -1 - K\exp(-\lambda D), \tag{3}$$

where we have introduced the dimensionless parameter K, which depends both on the total synaptic weight and on the slope of the f-I curve at the fixed point, $K=J\Phi'(I_{\text{ext}}-Jr_0)$. For small values of K, all eigenvalues have negative real parts and the network activity is time-independent. When K is increased, a pair of complex eigenvalues, $\lambda=\pm i\omega_c$, crosses the imaginary axis at a critical value $K=K_c$ signaling the onset of an oscillatory instability (i.e., a Hopf bifurcation). For $K>K_c$, the network activity follows a limit cycle and oscillates periodically. The critical K_c and the oscillation frequency at threshold are determined by Eq. (3),

$$1 + K_c \exp(-i\omega_c D) = -i\tau\omega_c. \tag{4}$$

Separating real and imaginary parts gives

$$\tan(\omega_c D) = -\tau\omega_c, \tag{5}$$

$$K_c = -\frac{1}{\cos(\omega_c D)}. \tag{6}$$

As the dimensionless ratio τ/D goes from 0 to $+\infty$, the oscillation threshold goes from 1 to $K_c \sim (\pi/2)\tau/D$ and the oscillation frequency goes from $\omega_c D=\pi$ to $\omega_c D=\pi/2$ (see Fig. 2).

This simple model thus predicts that the oscillation frequency is of the order of the inverse of the delay in the synaptic transmission. This can be simply understood since an increase in the network activity at time t results in an inhibitory input after the delay D and therefore a decrease in network activity at time $t+D$. This decrease itself provokes a lower inhibitory input after a second delay D and thus again a higher network activity at time $t+2D$. In this oscillatory regime, the dynamics at the single neuron level is modulated both at the neuron discharge frequency and at the collective oscillation frequency.

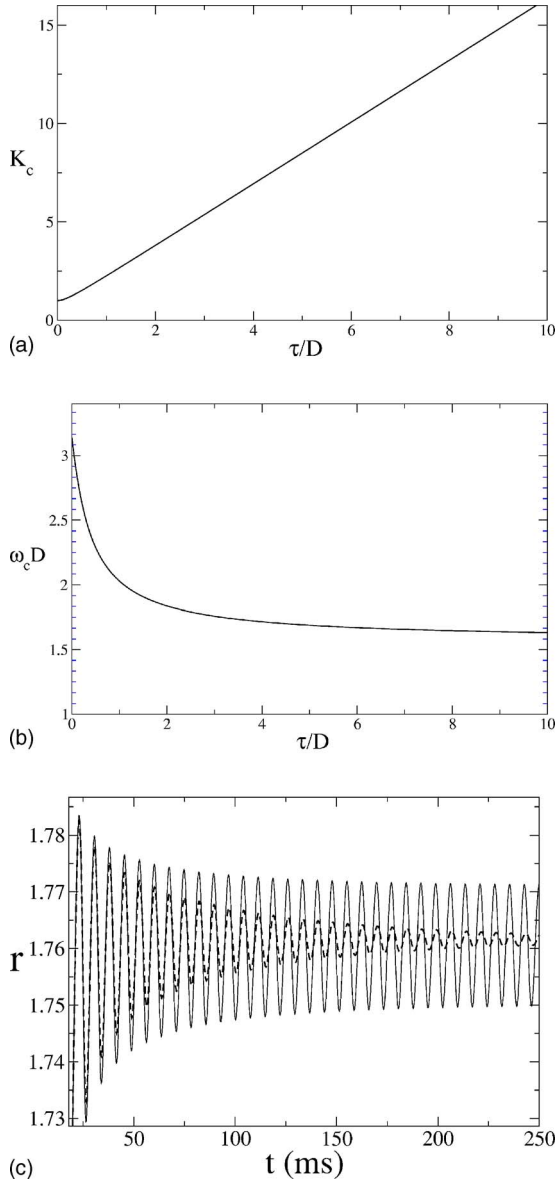

FIG. 2. (Color online) Oscillations in the rate model of Eq. (1). (a) Critical threshold K_c for oscillations. (b) Oscillation frequency ω_c at threshold. (c) Direct simulations of Eq. (1) with the f-I curve $\Phi(I)=1+\tanh(I)$, $\tau=10$ ms, and $D=2$ ms; for $\tau/D=5$, the linear threshold and frequency at threshold are $K_c \simeq 8.5$ and $\omega_c D=1.69$. For the two simulations shown, the rate at the fixed point $r_0=1.76$ and the total current $I_{\text{ext}}-Jr_0=1$ are identical. For $K=8.4$ (dashed line), the rate r relaxes toward the stable fixed point with damped oscillations. For $K=8.8$ (full line), r shows sustained oscillations with a period of 7.3 ms or $\omega D=1.73$.

Interestingly, the rate-model prediction relating the collective oscillation frequency to the characteristic of synaptic transmission holds in more realistic models. The rate model, however, does not allow for a quantitatively precise investigation of the effects of synaptic and neuronal dynamics on the properties of the oscillations. Hence, we now move to more realistic networks of spiking neurons.

III. FAST OSCILLATIONS IN NETWORKS OF SPIKING NEURONS

A. General formalism

The rate-model analysis described in Sec. II is a simple example of a self-consistent calculation of the model linear spectrum. More generally, the firing state can be written, similarly to the above calculation, as the steady firing rate r_0 plus a time-dependent small perturbation,

$$r(t) = r_0 + \mathrm{Re}[\hat{r}_1(\omega)\exp(i\omega t)]. \tag{7}$$

Although ω could be taken as a complex number (with $\omega=-i\lambda$ in the above calculation), for simplicity we will only consider real frequencies since this is sufficient to determine the oscillation threshold. Then, on the one hand, synaptic dynamics gives the recurrent network synaptic current as

$$I(t) = I_0 + \mathrm{Re}[\hat{I}_1(\omega)\exp(i\omega t)] \tag{8}$$

with

$$\hat{I}_1(\omega) = -JS(\omega)\hat{r}_1(\omega), \tag{9}$$

where the minus sign is due to the inhibitory nature of synapses, J measures the synaptic strength as precisely defined below [Eq. (17)], and $S(\omega)$ describes how synapses filter oscillatory presynaptic firing rates.

On the other hand, given a modulated injected current of the form (8), the neuron emits action potentials at the time-dependent rate (which depends on its intrinsic characteristics) of the form of Eq. (7) with

$$\hat{r}_1(\omega) = R(\omega)\hat{I}_1(\omega). \tag{10}$$

The consistency of Eqs. (9) and (10) provides the characteristic equation at threshold (since we restrict ourselves to real frequencies),

$$-JR(\omega)S(\omega) = 1. \tag{11}$$

Similarly, the modulus and phase of Eq. (11) provide two conditions that determine the linear threshold for the appearance of network oscillations and their frequency at threshold from the spike rate response $R(\omega)$ and the synaptic function $S(\omega)$. The phase of Eq. (11) shows in particular how the oscillation frequency is linked to the phase $\Phi_s(\omega)$ of the synaptic function $S(\omega)$ and to the phase $\Phi_R(\omega)$ of the spike response function,

$$\Phi_S(\omega) + \Phi_R(\omega) \equiv \pi \bmod[2\pi]. \tag{12}$$

Note that the oscillation frequency depends on the strength of the synaptic current only indirectly through its influence on the phase $\Phi_R(\omega)$ of the spike rate response.

We limit ourselves here to discuss the case in which the number of synapses on each neuron is sufficiently large so that the fluctuations in the mean synaptic current can be neglected. This is the case, for instance, of globally coupled networks in the limit of a large number of neurons, when individual couplings scale as $1/N$, where N is the size of the network. In sparsely coupled networks, when the size of individual couplings is $\gg 1/N$, the fluctuations in the synaptic current cannot be neglected and their amplitude is modulated at the network oscillation frequency. In some cases, their effect can be included along lines similar to the present discussion by introducing still another function, the spike rate response to a modulated current variance (see, e.g., Refs. 6 and 23).

The first simplification in the rate-model description was to take the synaptic current as simply proportional to a delayed copy of the network activity,

$$S_D(\omega) = \exp(-i\omega D). \tag{13}$$

A second, conceptually more important, approximation was to obtain the firing rate response to an oscillating current from the derivative of the f-I curve as

$$R_{rm}(\omega) = \frac{\Phi'(I_0)}{1 + i\omega\tau}. \tag{14}$$

We discuss now how S and R are modified when more realistic synaptic and neuronal models are introduced.

B. A more realistic description of synaptic currents: Latency, rise, and decay times

A common description of the synaptic current involves a rise time τ_r, a decay time τ_d, and a latency τ_l (see, e.g., Refs. 9 and 24). When the presynaptic neuron emits a spike at time t_s, the post-synaptic current (PSC) is increased by

$$I_{\rm syn}(t) = -\frac{J_s}{\tau_d - \tau_r}\left[\exp\left(-\frac{t-(t_s+\tau_l)}{\tau_d}\right)\right] - \exp\left(-\frac{t-(t_s+\tau_l)}{\tau_r}\right)\theta(t-t_s-\tau_l), \tag{15}$$

where $J_s > 0$ is the strength of individual synaptic connections and the minus sign comes from our consideration of inhibitory synapses. The modulation of the mean synaptic current entering a cell receiving inputs from N_s synapses described by Eq. (15) follows that of the mean network firing rate $r(t)$ for weak modulations. With the notations of Eqs. (7) and (8), one obtains

$$I = I_0 + [\hat{I}_1 \exp(i\omega t) + \text{c.c.}]$$

with

$$I_0 = I_{\rm ext} - N_s J_s r_0,$$
$$\hat{I}_1 = -N_s J_s \hat{r}_1 \frac{\exp(-i\omega\tau_l)}{(1+i\omega\tau_r)(1+i\omega\tau_d)}. \tag{16}$$

We define $N_s J_s$ as the total synaptic strength J,

$$J = N_s J_s. \tag{17}$$

Hence, the modulated current is related to the network rate modulation by

$$S(\omega) = \frac{\exp(-i\omega\tau_l)}{(1+i\omega\tau_r)(1+i\omega\tau_d)}, \tag{18}$$

which can be compared to the synaptic response [Eq. (13)] of the simplest rate model of Sec. II. The inhibitory synaptic current lags behind the firing rate with a phase $\pi + \Phi_S(\omega)$ with, from Eq. (18),

$$\Phi_S(\omega) = -\omega\tau_l - \arctan(\omega\tau_r) - \arctan(\omega\tau_d). \tag{19}$$

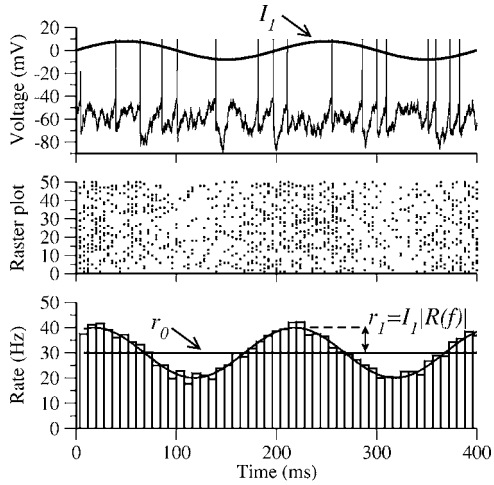

FIG. 3. Sketch of the spike response rate $R(\omega)$. A small oscillatory current is added on top of inputs that elicit firing at a steady rate r_0. This results in a modulation of the instantaneous network firing rate that is linearly proportional to the amplitude of the oscillatory current and that depends on its frequency $f = \omega/2\pi$.

C. Spike rate response

In the rate-model description, the response of a neuron to an oscillating current was directly related to the derivative of its f-I curve [Eq. (14)]. This relationship actually holds for any model neuron for a sufficiently low drive frequency when the firing rate has enough time to relax to the oscillatory drive,

$$\lim_{\omega\to 0} R(\omega) = \Phi'(I_0). \tag{20}$$

However, for arbitrary frequencies ω the spike rate response $R(\omega)$ is in general independent of the steady-state f-I curve. This function $R(\omega)$ measures the mean instantaneous firing rate modulation of a neuron submitted to an oscillatory drive. This is schematically depicted in Fig. 3: identical independent neurons under steady and, in general, noisy conditions are given an identical small oscillatory drive. The spike rate response is a linear response function: as defined in Eq. (10), $R(\omega)$ measures the small *modulation* of the instantaneous firing rate at the driving frequency [note that the change in the steady firing rate when the neuron is submitted to the oscillatory drive vanishes at the linear level and is not measured by $R(\omega)$].

The importance of the spike rate response, and especially its phase, for the occurrence of network oscillations and their frequency, has motivated the computations of $R(\omega)$ for different model neurons under several driving conditions.

1. Leaky-integrate-and-fire (LIF) neurons submitted to white noise (WN)

The LIF neuron is one of the simplest models of a spiking neuron.[25–27] Its dynamics is given by

$$\tau\frac{dV}{dt} = -V + I(t), \tag{21}$$

where V represents the departure of the membrane potential from the resting potential and $I(t)$ is the injected current. In

order to model spike emission, threshold and reset potentials are added to this linear description of a membrane with passive resistance and capacity. When V reaches a threshold potential V_T, a spike is emitted, and the potential is reset to V_R after a refractory period $\tau_{\rm rp}$. The spike rate response $R(\omega)$ can be obtained analytically when $I(t)$ is a sum of a constant current and a white noise term,

$$I = I_0 + \sigma\sqrt{\tau}\eta(t), \tag{22}$$

with $\langle \eta(t)\eta(t')\rangle = \delta(t-t')$. In this case, computing the spike rate response rate corresponds to evaluating the linear firing rate modulation resulting from an additional small oscillatory current $[\hat{I}_1 \exp(i\omega t)+\text{c.c.}]$. This can be done analytically using a Fokker-Planck equation to describe the distribution of subthreshold potentials of the ensemble of neurons.[6] The spike response rate is obtained as

$$R_{\rm LIFWN}(\omega) = \frac{r_0}{\sigma(1+i\omega\tau)}\left(\frac{\frac{\partial U}{\partial y}(y_t,\omega\tau) - \frac{\partial U}{\partial y}(y_r,\omega\tau)}{U(y_t,\omega\tau) - U(y_r,\omega\tau)}\right), \tag{23}$$

where the parameter y_t and y_r are related to the threshold and reset potential and U can be expressed as a linear combination of standard hypergeometric functions,[28]

$$y_t = \frac{V_T - I_0}{\sigma}, \quad y_r = \frac{V_R - I_0}{\sigma}, \tag{24}$$

$$U(y,w) = \frac{e^{y^2}}{\Gamma[(1+iw)/2]} M\left(\frac{1-iw}{2}, \frac{1}{2}, -y^2\right) + \frac{2ye^{y^2}}{\Gamma(iw/2)} M\left(1-\frac{iw}{2}, \frac{3}{2}, -y^2\right).$$

In particular, at high frequencies the spike rate modulation amplitude lags by 45 degrees behind the current drive and decreases like the inverse square root of the frequency,

$$R_{\rm LIFWN} \sim \frac{r_0}{\sigma}\sqrt{\frac{2}{\omega\tau}}\exp\left(-i\frac{\pi}{4}\right). \tag{25}$$

2. Leaky-integrate-and-fire (LIF) neurons submitted to correlated noise (CN)

Synapses filter noise. It is therefore interesting to know how the results (23) and (25) are modified when the noise is colored instead of being white. One can first introduce the synaptic current decay time since rise times are usually much faster. This amounts to replacing Eq. (22) by

$$\tau_d \frac{dI}{dt} = -I + \sigma\sqrt{\tau}\eta(t), \tag{26}$$

where $\eta(t)$ is a white noise as before. In this case, the spike rate response is not known in exact form, but it can be obtained in perturbation in the limit where the synaptic decay time is short as compared to the membrane time constant $\tau_d \ll \tau$. In particular, the high-frequency limit of this first-order term (in an expansion in $\sqrt{\tau_d/\tau}$) is real and constant,[12,13]

$$R^{(1)}_{\rm LIFCN} \sim 1.32\frac{r_0}{\sigma}\sqrt{\frac{\tau_d}{\tau}}. \tag{27}$$

Thus, in the presence of colored noise, the spike rate response neither vanishes nor lags behind the current drive at high frequency. This remains true for larger values of $\sqrt{\tau_d/\tau}$ and numerical simulations have shown that there is a smooth crossover between Eq. (27) and the other limit where $\sqrt{\tau_d/\tau}$ is large and noise vanishes.[13] Finally, the effect of a finite synaptic rise time can be well accounted for in a phenomenological way, by substituting in the zero rise time results τ_d by $\tau_d+\tau_r$ (as is suggested by computing the standard deviation of the fluctuating current).

3. Conductance-based models and nonlinear integrate-and-fire (NLIF) neurons

A simplification of the integrate-and-fire model lies in its sharp threshold for spike emission that replaces the opening with depolarization of sodium voltage-gated channels in more realistic conductance-based descriptions (and in real neurons). Numerical simulations have been performed to assess the influence of the spike generation mechanism on the spike response rate.[14] The results were found to be well-accounted for by replacing the sharp threshold of the LIF model by a smoother exponential nonlinearity. That is, taking instead of Eq. (21) the exponential-integrate-and-fire (EIF) model,

$$\tau\frac{dV}{dt} = -V + \psi(V) + I(t), \tag{28}$$

with

$$\psi(V) = \Delta_T \exp\left(\frac{V-V_T}{\Delta_T}\right). \tag{29}$$

The threshold is taken to be infinite since, for a suprathreshold input current ($I>0$), the nonlinearity $\psi(V)$ drives the potential to infinity in a finite time. After spike emission, the potential is reset to V_R as for the LIF. The spike response rate of the EIF model matches well that of the conductance-based Wang-Buzsáki model.[4] The smooth spike generation mechanism leads the spike rate response to decrease faster at high frequency than the LIF response function,

$$R_{\rm EIF} \sim \frac{r_0}{\Delta_T\omega}\exp\left(-i\frac{\pi}{2}\right) \tag{30}$$

Namely, the spike rate modulation decreases as $1/\omega$ at high frequency and lags behind the current drive by 90 degrees for both white noise and correlated noise. For a small Δ_T, the spike initiation is sharp and the asymptotic behavior (30) is only reached at very high frequencies. The LIF behaviors [Eq. (25) or Eq. (27)] are then observed in an intermediate frequency range.

We note here that the spike rate response of the quadratic-integrate-and-fire neuron [that is, with $\psi(V) \propto V^2$] has also been studied. It decreases at high frequencies like ω^{-2} and with a phase lag of 180 degrees with respect to the oscillatory current drive.

4. Generalized integrate-and-fire neurons with subthreshold resonance

Besides its simplified spike mechanism, the LIF purely passive subthreshold dynamics does not match what is observed in certain types of neurons. Subthreshold resonance is one such phenomenon that has been analyzed because of its direct relevance to oscillatory behavior. It has been found in several experiments that the subthreshold response of some neurons subjected to a small oscillatory current drive exhibited a peak at a particular frequency. This resonance is not present in the LIF model. The simple RC-circuit membrane produces a voltage response that decreases monotonically as a function of the input current frequency. The membrane resonance depends on the particular combination of ionic channels expressed by the neurons, but it can be accurately described by a simple generalization of the LIF model. This generalized integrate-and-fire (GIF) model simply consists in adding one supplementary variable to the basic LIF description and reads[15]

$$\tau \frac{dV}{dt} = -V - \gamma W + I(t),$$
$$\tau_1 \frac{dW}{dt} = W - V. \tag{31}$$

The additional variable W accounts for the voltage-gated current that flows into the cell. A variable W that opposes voltage change ($\gamma > 0$) is sufficient to create a subthreshold resonance when τ_1 is a few times longer than τ.[15,29] In the same conditions, the additional variable W allows the spike response rate to *phase advance* with respect to an oscillatory current drive that has a frequency close to the subthreshold resonance, but only when the noise in the drive is strong enough.[15,16] In principle, this phase advance should allow for sparsely synchronized oscillations of recurrent networks of excitatory cells close to the subthreshold frequency. The impact of subthreshold resonance on network dynamics is the subject of current investigation.

D. Inhibitory networks in the sparsely synchronized oscillatory regime: Some examples

The simplest example of application of the above formalism is a network of N globally coupled inhibitory LIF neurons when each one is submitted in addition to a constant current I_{ext} and a strong white noise of amplitude σ independent from neuron to neuron, as in Fig. 1. The mean current I entering a neuron is the sum of the external current and the average recurrent synaptic current as given by Eq. (16). The steady discharge rate and I_0 should first be determined self-consistently (since the recurrent part of the entering current depends on the discharge rate, which itself is determined by the entering current) as for the rate model Eq. (2). Once I_0 is determined, the exact result of Eq. (23) can be directly applied. For sufficiently strong noise, the phase $\Phi_R(\omega)$ is a function that decreases monotonically from 0° at low frequencies [from Eq. (20)] to −45° [Eq. (25)] at high frequencies. The phase of the spike rate response $\Phi_R(\omega)$ together with the phase of $S(\omega)$ determine the oscillation frequency at threshold with

$$\omega_c \tau_l + \arctan(\omega_c \tau_r) + \arctan(\omega_c \tau_d) = \pi + \Phi_R(\omega_c), \tag{32}$$

where we have taken the relevant branch at high noise of Eq. (12) (the other branches are briefly discussed in Sec. IV). For fast oscillations in a network of LIF neurons, $\Phi_R(\omega)$ tends toward $-\pi/4$ and the oscillation frequency depends only on the synaptic current time constants. For instance, when $\tau_r = \tau_d = 0$, and only a finite latency τ_l is kept (δ-function synaptic current), one obtains $\omega_c \sim 3\pi/(4\tau_l)$ in the limit of short latencies [to be compared to $\omega_c \sim \pi/(2D)$ for the rate model in the same limit]. A more realistic case in which the three synaptic time constants are nonzero is shown in Fig. 1. In this case, the network frequency is the particular frequency for which the monotonically increasing left-hand side of Eq. (32) is equal to $3\pi/4$. In the example of Fig. 1, it is found to be about 90 Hz, in good agreement with numerical simulations. When the neurons are subject to colored noise, $\Phi_R(\omega)$ vanishes at high frequencies and this leads to higher oscillation frequencies for the same synaptic parameters.

The effect of intrinsic properties of neurons on network oscillations can be understood along the same lines, through their effects on the phase lag of the instantaneous firing rate with respect to an oscillatory input. In general, intrinsic ionic currents can be separated in two classes. (i) Intrinsic currents that provide negative feedback on membrane potential, such as adaptation currents, or currents leading to subthreshold resonance (slow K^+, H).[29] As shown in Sec. III C 4, these currents typically lead to a *phase advance* of neuronal response at *low* frequencies (low compared to the time scale of the involved currents).[15,30] The intuitive picture is that these currents tends to oppose slow variations in the membrane potential and/or instantaneous firing rate. Hence, these currents potentially generate other oscillatory modes in which frequency could be primarily determined by intrinsic properties.[30] Another effect of such currents could be to amplify network oscillations if intrinsic and network frequencies match. (ii) Intrinsic currents that provide positive feedback on the membrane potential, leading to spike initiation (fast Na^+ current). As shown in Sec. III C 3, these currents control the neuronal response at high frequency, introducing an additional phase shift at high frequencies compared to a leaky integrate-and-fire neuron.[14] This additional phase shift potentially decreases network frequency in fast oscillatory regimes.[10,11]

E. From weak to strong noise

As emphasized in the preceding sections, the stochastic synchronous oscillations depend on a real or "effective" noise source—either external noise or neuron-to-neuron fluctuations induced by random network connectivity. In the absence of noise and disorder in synaptic connectivity, networks of spiking neurons typically settle in states in which neurons fire periodically. The network itself can be either asynchronous or synchronized in one or several clusters of synchronously firing neurons.[5,31–42] A question then is, what happens when one increases the noise level, starting from

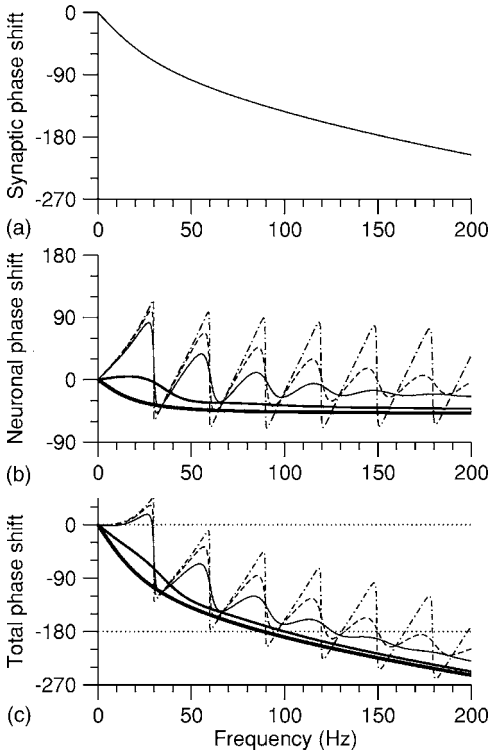

FIG. 4. Interpretation of Eq. (11) in terms of synaptic and neuronal phase shifts. (a) Synaptic phase shift, $-\omega\tau_l-\arctan(\omega\tau_r)-\arctan(\omega\tau_d)$, as a function of the frequency f, for $\tau_l=1$ ms, $\tau_r=1$ ms, and $\tau_d=6$ ms. (b) Neuronal phase shift, $\Phi_R(2\pi f)$, for $V_t=20$ mV, $V_r=14$ mV, $\nu_0=30$ Hz, $\tau_m=10$ ms, and five noise levels: 0.01 mV (dot-dashed line), 0.05 mV (dashed line), 0.1 mV (thin solid line), 1 mV (medium solid line), and 10 mV (thick solid line). Note the sharp variations at integer multiples of the firing rate ν_0 (30, 60, 90,… Hz) for low noise levels, that disappear as noise becomes stronger. (c) Total phase shift [sum of synaptic and neuronal phase shifts, for the same noise levels as in (b)]. Solutions to Eq. (32), for a given noise level, are at the intersection of the curve representing the total phase shift and the horizontal dotted line at −180 degrees. Note the large number of intersections for low noise levels that disappear as noise increases until a single intersection is left. Adapted from Ref. 11.

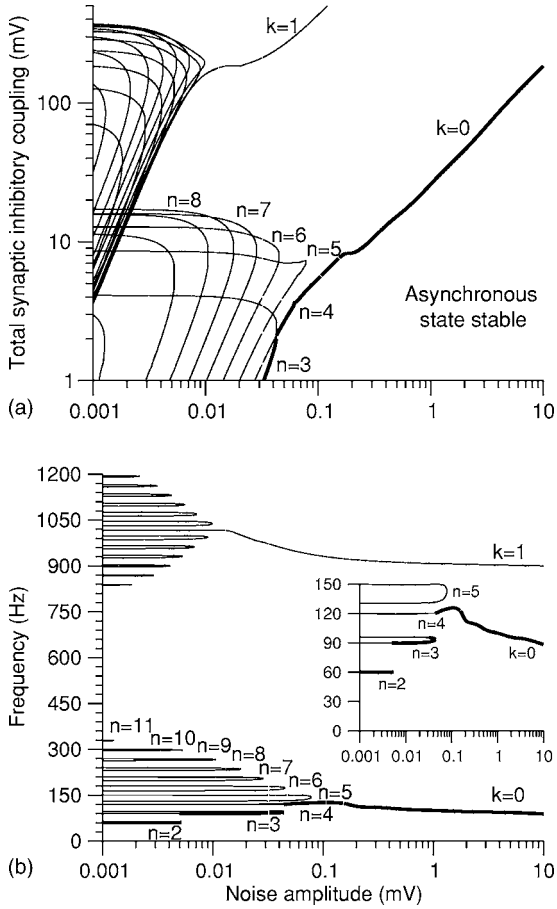

FIG. 5. (a) Lines on which eigenmodes become unstable, obtained from Eq. (11), in the plane J-σ, for the parameters of Fig. 4. The asynchronous state is stable below the lowest line (region marked "asynchronous state stable"). Several solutions of families to Eq. (11) exist, and are indexed by an integer k such that $\Phi_S(\omega)+\Phi_R(\omega)+(2k+1)\pi=0$. Only lines corresponding to families of solutions at $k=0$ and $k=1$ (marked in the figure) are indicated. Each family is composed of individual branches labeled by integer values of n (indicated only for $k=0$). (b) Frequency of marginal modes. The thick curve in (a) is the stability boundary of the asynchronous state. The thick curve in (b) is the frequency of the unstable mode on this boundary plotted against the noise. Adapted from Ref. 11.

either the "cluster" states at zero noise or the stochastic oscillations at large noise? This question was addressed in a recent study of the dynamics of a fully connected network of inhibitory neurons with external noise.[11]

A key to understanding the differences between small noise and large noise regimes is to study the behavior of the phase shift of a single neuron instantaneous firing rate in response to oscillatory inputs. As shown by several studies, the response of the instantaneous firing rate $R(\omega)$ depends markedly on the level of noise: at low noise levels, the amplitude of the firing rate modulation exhibits pronounced resonances at the firing frequency of the neuron and at its harmonics (integer multiples of the firing frequency).[12,26,39] As the amplitude of the noise increases, these peaks disappear progressively (the higher harmonics disappearing earlier), until at some critical value of noise the amplitude decays monotonically with frequency. A similar behavior is observed with the phase, as shown in Fig. 4. At low noise levels, the phase versus frequency curve exhibits a seesaw behavior: the phase decreases sharply at the firing frequency and at its integer multiples, while it increases smoothly in intervals in between two successive integer multiples. As a result, there is an odd number $2n+1$ of solutions of Eq. (11) that satisfy $\Phi_S(\omega)+\Phi_R(\omega)+\pi=0$, out of which $n+1$ are very close to integer multiples of the firing frequency. Such instabilities lead to cluster states, where the number of clusters is determined by the ratio (frequency of the instability)/(firing frequency). On the other hand, when the noise is large, the "teeth" in the phase versus frequency curve disappear progressively, and the phase now varies smoothly between its low- and high-frequency limits. This dependence is monotonic in the case of white noise. Consequently, there is only a single solution to Eq. (11); this solution has no longer any relationship with the firing frequency or any of its integer multiples.

Figure 5 shows the region of stability of the asynchronous state in the J-σ plane, together with the various instability lines in this plane. Patterns of activity for various

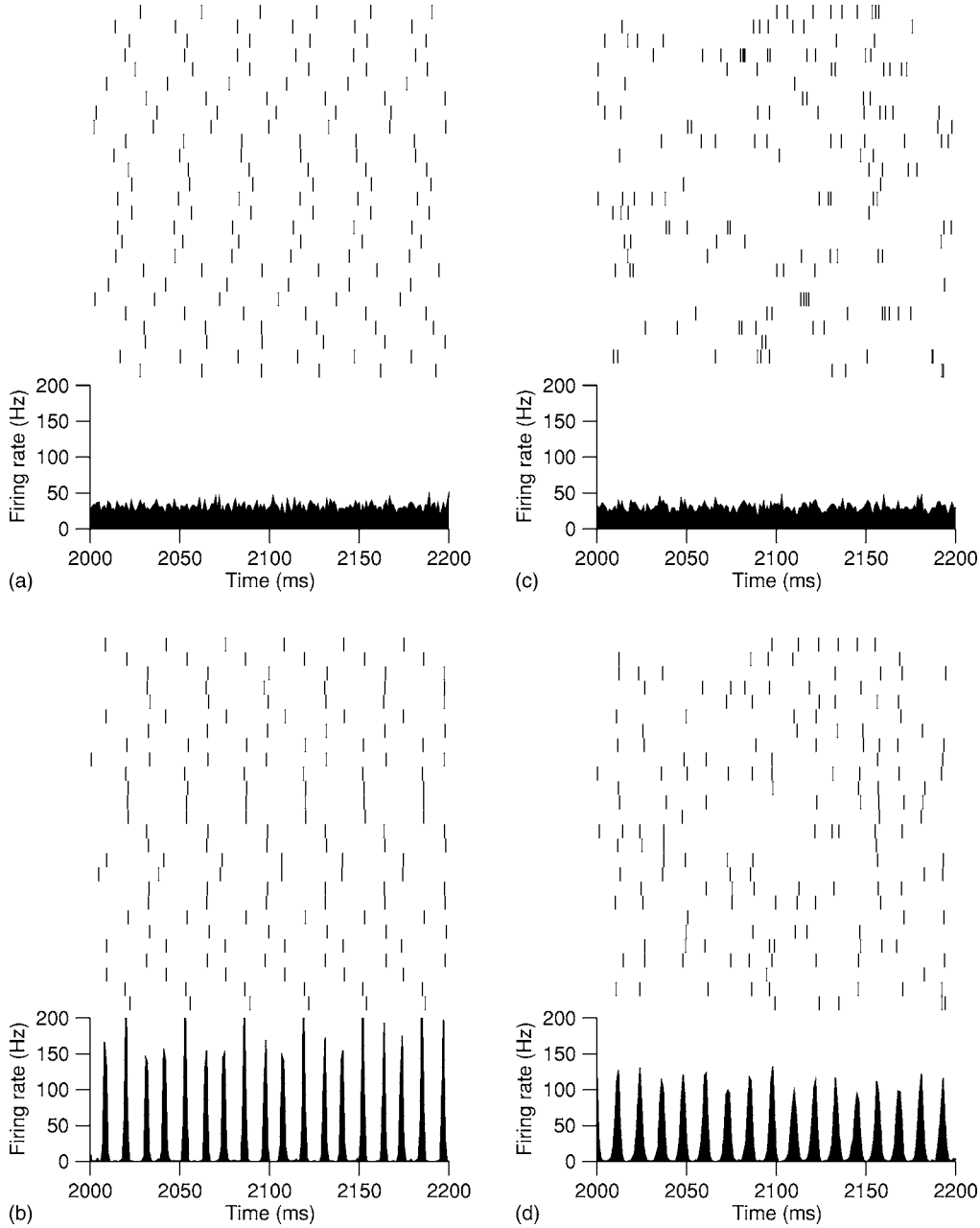

FIG. 6. Simulations of a network of 1000 LIF neurons. All four panels show spike trains of 20 selected neurons (rasters) and instantaneous population firing rate, computed in 1 ms bins. [(a) and (b)] Low coupling/low noise region. In panel (a), the asynchronous state is stable ($J=1$ mV, $\sigma=0.04$ mV). In (b), the noise is decreased ($\sigma=0.02$ mV). The network now settles in a three-cluster state, as predicted by the analytical results. [(c) and (d)] Strong coupling/strong noise region. (c) $J=100$ mV, $\sigma=10$ mV; the asynchronous state is stable. Decreasing σ to $\sigma=4$ mV leads to a stochastic oscillatory state, as predicted by the analytical results. Adapted from Ref. 11.

coupling strengths and noise amplitudes are illustrated in Fig. 6.

Finally, it is instructive to consider the single neuron membrane potential dynamics in different oscillatory regimes, as noise and coupling strength are varied (see Fig. 7). For very low coupling strength and noise, the network settles in a cluster state in which neurons fire almost periodically with a frequency that is smaller than the network frequency [by a factor 3 in Fig. 7(a)]. The coupling is so weak that the inhibitory feedback from the synchronized clusters to which the neurons do not participate is almost unnoticeable. Increasing both coupling strength and noise, one reaches a state in which the oscillatory feedback from the network significantly modifies the single cell voltage [Fig. 7(b)]. A clear subthreshold oscillation is visible, with the neuron spiking once every few cycles of this oscillation. In this regime, the voltage trace resembles that of a single cell model exhibiting mixed-mode oscillations (see, e.g., Ref. 18). Finally, at even larger coupling strength and noise, subthreshold oscillations become barely visible in the membrane potential dynamics even though the network exhibits pronounced oscillations, and the cell fires in a very irregular fashion in a small fraction of cycles [Fig. 7(c)].

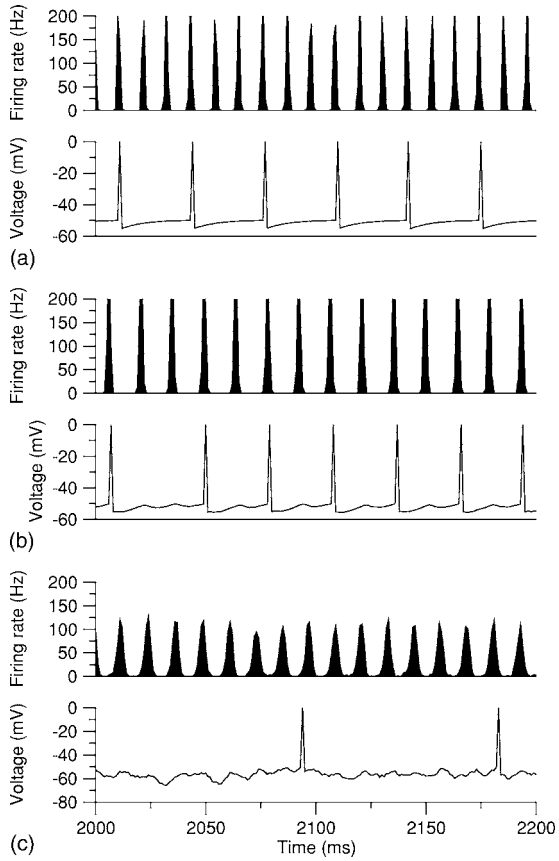

FIG. 7. Comparison between single neuron voltage dynamics in three oscillatory regimes. In all three cases, the global network activity is shown as the top graph, and the membrane potential of a single neuron as the bottom graph. (a) Low coupling/low noise ($J=1$ mV, $\sigma=0.02$ mV): spike emission is locked to the collective oscillation with different phases for neurons in different clusters. However, the coupling is weak enough that spike emission in the other clusters cannot be seen in the shown membrane potential trace. (b) Intermediate coupling/intermediate noise ($J=20$ mV, $\sigma=0.3$ mV): this regime is quite similar to the previous one but stronger noise makes jumps between different locked states more frequent (one can be seen at the beginning of the shown membrane potential trace). Moreover, stronger coupling makes clearly visible on the membrane potential the spike emission of the other clusters. In this regime, the coexistence of spikes and small periodic deflections in the single neuron membrane potential leads to a strong resemblance to MMO oscillations in single cell models. (c) Strong coupling/strong noise ($J=100$ mV, $\sigma=4$ mV): noise is strong enough so that spike emission is not locked to the collective oscillation and very noisy. Clusters no longer exist.

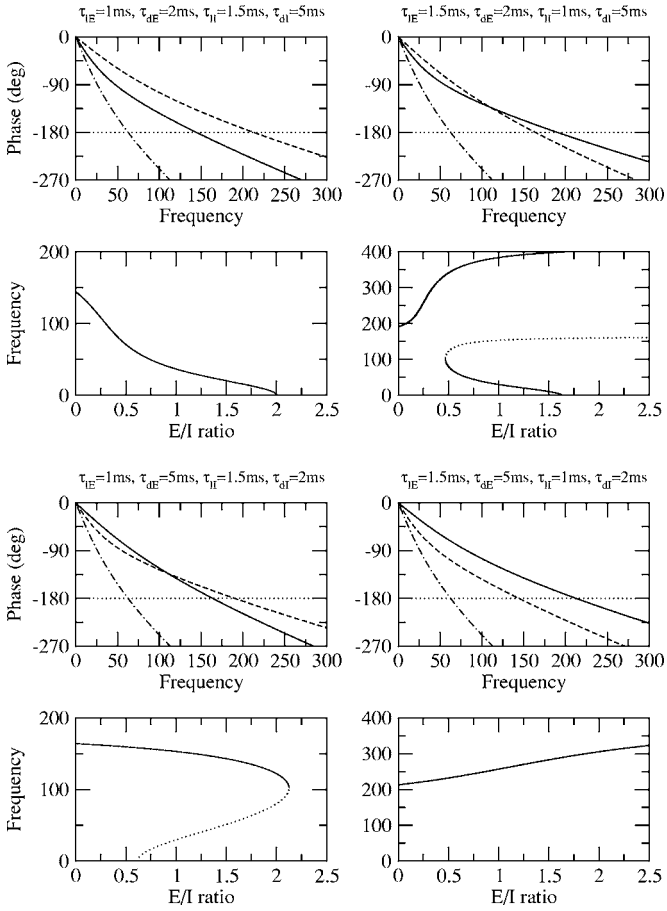

FIG. 8. Effect of excitation/inhibition balance on network frequency, for four different sets of synaptic time constants, indicated on top of the phase vs frequency panels (rise times are 0.5 ms in all panels). For each set, we show the synaptic phase shift of inhibitory (solid) and excitatory (dashed) synapses, together with the sum of the two (dot-dashed). The intersection of the solid curve with the horizontal dotted line indicates the frequency of a purely inhibitory network, while the intersection of the dot-dashed curve and the dotted line indicate the frequency of a network with E-I loop only. We also show how the network frequency depends on the E/I ratio α. Note the different qualitative behaviors as a function of relative time constants. Top left: excitation is faster than inhibition: frequency decreases with E/I ratio. Top right: inhibition has shorter latency but longer decay time: frequency first increases, then jumps discontinuously to a much lower (<100 Hz) frequency, and then decreases. Bottom left: inhibition has longer latency but shorter decay time, frequency decreases with E/I ratio. Bottom right: inhibition is faster than excitation: frequency increases with E/I ratio.

IV. EXCITATORY-INHIBITORY NETWORKS

We have considered so far purely inhibitory networks. What happens when excitatory neurons are coupled to the network of inhibitory neurons? It is well known that the excitation-inhibition feedback loop is another potential mechanism for generating network oscillations. Consider indeed an excitatory-inhibitory network in which the only connections that are present are excitatory synapses onto interneurons and inhibitory synapses onto excitatory cells (no mutual excitation, no mutual inhibition). It is then easy to show that oscillations appearing on an instability of the asynchronous state have a frequency that obeys the equation[9,10]

$$\Phi_{RE}(\omega)+\Phi_{SE}(\omega)+\Phi_{RI}(\omega)+\Phi_{SI}(\omega)=\pi, \tag{33}$$

in which $\Phi_{RE}(\omega)$ and $\Phi_{RI}(\omega)$ represent the phase shift of the firing rate of excitatory (E) and inhibitory (I) neurons with respect to an oscillatory drive, and $\Phi_{SE}(\omega)$ and $\Phi_{SI}(\omega)$ correspond to the phase shift induced by excitatory (E) and inhibitory (I) synapses. Hence, the frequency of the oscillation depends on the time course of both excitatory and inhibitory PSCs, and on the ability of both inhibitory and excitatory neurons to follow an oscillatory drive. In particular, in case the phase shift of both interneurons and pyramidal cells can be neglected, the frequency of the oscillation becomes

$$\Phi_{SE}(\omega)+\Phi_{SI}(\omega)=\pi. \tag{34}$$

One notices from Eq. (34) that since $\Phi_{SE}>0$, the E-I loop has a frequency that is necessarily slower than the oscillation frequency induced by mutual inhibition (I-I loop).[9,10] This is shown graphically in Fig. 8. For the synap-

tic time scales chosen in Fig. 8 the frequency is in the range 150–250 Hz for a pure I-I mechanism, while it drops to about 60 Hz for the E-I mechanism.

More generally, oscillations in E-I networks can be due to a mixture of the two mechanisms, depending on the relative strength of the E-I loop and of the I-I loop. Mathematically, the oscillation frequency can be obtained by solving the equation

$$[1 + J_{II}R_I(\omega)S_I(\omega)][J_{EE}R_E(\omega)S_E(\omega) - 1] = J_{EI}J_{IE}R_I(\omega)R_E(\omega)S_E(\omega)S_I(\omega), \quad (35)$$

where J_{EE}, J_{IE}, J_{EI}, and J_{II} measure the strength of the interactions between E and I populations.

Apart from the already discussed cases $J_{EE}=J_{EI}=J_{IE}=0$ (mutual inhibition) and $J_{EE}=J_{II}=0$ (E-I loop), another case of interest is when the balance between excitation and inhibition is the same onto excitatory and inhibitory cells, i.e., $J_{EE}/J_{EI}=J_{IE}/J_{II}=\alpha$. Neglecting again the neuronal phase shifts of both populations allows us to focus on how the parameter α affects the network frequency, for various values of the synaptic time constants. In the case in which excitatory and inhibitory synaptic time constants are identical,[7] the network frequency is unaffected by the E/I ratio. Figure 8 shows that depending on the relative values of excitatory and inhibitory latencies and decay times, the network frequency can either increase or decrease as a function of E/I ratio. The dependency can be even nonmonotonic when inhibition has shorter latency but longer decay time: the frequency first increases, then jumps abruptly to a much lower frequency, and then decreases continuously.[10] Hence, depending on the E/I balance, a network can oscillate at widely different frequencies.

V. THEORY VERSUS EXPERIMENT

Networks of the brain produce oscillations with a wide diversity of frequencies and degrees of coherence. In this paper, we have addressed mechanisms of oscillations induced primarily by synaptic characteristics, which typically give rise to fast oscillations (in the gamma range or faster). Slower oscillations observed in the brain are likely to depend on other mechanisms such as cellular pacemaker mechanisms (see, e.g., Ref. 43 for a review). In such slower rhythms (e.g., delta, theta, etc.), the firing rate of single cells is no longer lower, and can in fact be larger, than the network frequency. Strongly modulated firing rates based on interactions between different populations have also been described, as, for example, in the generation of sleep spindle waves.[44] In the following, we restrict ourselves to fast oscillations and survey briefly experimental data on some good candidates for fast sparsely synchronized oscillations. More detailed surveys of data on fast oscillations can be found in several recent reviews.[45,46]

A. Hippocampal sharp waves

Among the numerous patterns of oscillatory activity recorded in the hippocampus of the rat, the fastest rhythm are the "ultrafast ripple" oscillations (140–200 Hz). These oscillations are associated with "sharp waves" in the CA1 area and occur during awake immobility, consummatory behaviors, and slow-wave sleep.[19,47,48] Single neuron behavior during such episodes is entirely consistent with a stochastic oscillation mechanism, since both pyramidal cells and interneurons fire at a much lower rate than the population oscillation (pyramidal cells: 8 Hz; interneurons: 30 Hz).[19]

B. Fast oscillations in the cerebellum

Fast oscillations were first recorded in the cerebellum by Adrian.[49] Recently, de Solages *et al.*[50] have recorded the activity of individual Purkinje cells, the inhibitory neurons that form the sole output of the cerebellar cortex, together with the local field potential (LFP) in anesthetized rats. The oscillations were found to share all the characteristics of the fast oscillations described here: fast (150–250 Hz) oscillations of the LFP together with Purkinke cells firing at an average of 38 Hz. Furthermore, pharmacological experiments indicated that the underlying mechanism involved the Purkinje axon collaterals, in agreement with the model.

C. Gamma oscillations

Gamma oscillations are observed *in vivo* in the neocortex[51,52] and the hippocampus[53] of awake behaving animals, as well as in *in vitro* preparations using agonists of the acetylcholine receptor and/or kainate receptors.[54,55] In both *in vivo* and *in vitro* studies, pyramidal cells fire irregularly at much lower rates than the frequency of the global oscillation. However, the picture is less clear concerning inhibitory neurons.

In at least one *in vitro* study, two identified classes of interneurons fire approximately once (occasionally twice) per cycle, indicating a strongly synchronized regime.[56] Two other *in vitro* studies report firing rates, CVs, and ISI distributions consistent with sparsely synchronized oscillations.[57,58] The picture *in vivo* is less clear, though correlation of firing probability and of field potential seems consistent with a weak synchronization regime.[53,59] It seems plausible that depending on the level of noise and external inputs, networks of the hippocampus can be in different synchronized states. Strongly synchronized states would tend to be more prevalent *in vitro* where the noise levels are usually much smaller than *in vivo*.

Gamma oscillations occur also in the olfactory bub.[2,60] A recent experimental and simulation study[61] proposed to model the particular connectivity of the olfactory bulb as an effective inhibition between the principal mitral cells. The LFP and the discharge patterns of the mitral cells have then similar characteristics to the sparsely synchronized regime described here.

VI. CONCLUSIONS

In this paper, we have discussed the properties of fast sparsely synchronized oscillations, starting from a simple rate model. The formalism developed in Sec. III was shown to be very general (provided a network is large enough) and to apply to networks of integrate-and-fire neurons, but also to networks of neurons incorporating more biophysically realistic features.[8,10,11,30]

At least one other mechanism has been proposed for generating fast oscillations, namely axo-axonal gap junctions between pyramidal cells.[62,63] This scenario is able to account for fast oscillations that occur in the absence of chemical synaptic transmission in slices.[64,65] However, the existence of such an axo-axonal gap junction remains the subject of debate. Subthreshold membrane oscillations with sparse firing on top of these oscillations can also be generated at the single cell level.[18,66]

Finally, here as in most previous studies, we have focused on local networks in which the connection probability is identical between cell pairs. Recently, the effect of spatial structure on network dynamics was studied in Ref. 67 using a ring architecture. A large variety of spatio-temporal patterns was uncovered beyond the homogeneous fast oscillations discussed here: localized oscillations in which two bumps oscillate in antiphase, chaotic states occurring through a cascade of period-doubling bifurcations, traveling waves, lurching waves, etc. In addition, such networks exhibit bistability between various patterns in numerous regions of parameter space. The analysis of spatially structured networks thus appears to be a rich field for future studies. Further experimental and theoretical studies will also be necessary to assess the functional significance of fast neural oscillations (spatially structured or not), which remains to be clarified, in spite of suggestive proposals.[68]

ACKNOWLEDGMENTS

It is a pleasure to take the opportunity of this brief survey to thank the numerous persons with whom we have discussed this topic over the past years, and especially our collaborators D. Amit, B. Barbour, S. Dieudonné, G. Dugué, N. Fourcaud, C. Geisler, D. Hansel, C. Léna, M. Richardson, C. de Solages, C. van Vreeswijk, and X. J. Wang. We also thank H. Rotstein for useful comments on the manuscript.

[1]H. Berger, Arch. Psychiatr. Nervenkr. **87**, 527 (1929).
[2]E. D. Adrian and B. H. C. Matthews, Brain **57**, 355 (1934).
[3]C. van Vreeswijk, L. Abbott, and G. B. Ermentrout, J. Comput. Neurosci. **1**, 313 (1994).
[4]X.-J. Wang and G. Buzsáki, J. Neurosci. **16**, 6402 (1996).
[5]D. Hansel, G. Mato, and C. Meunier, Neural Comput. **7**, 307 (1995).
[6]N. Brunel and V. Hakim, Neural Comput. **11**, 1621 (1999).
[7]N. Brunel, J. Comput. Neurosci. **8**, 183 (2000).
[8]P. H. Tiesinga and J. V. Jose, Network **11**, 1 (2000).
[9]N. Brunel and X.-J. Wang, J. Neurophysiol. **90**, 415 (2003).
[10]C. Geisler, N. Brunel, and X.-J. Wang, J. Neurophysiol. **94**, 4344 (2005).
[11]N. Brunel and D. Hansel, Neural Comput. **18**, 1066 (2006).
[12]N. Brunel, F. Chance, N. Fourcaud, and L. Abbott, Phys. Rev. Lett. **86**, 2186 (2001).
[13]N. Fourcaud and N. Brunel, Neural Comput. **14**, 2057 (2002).
[14]N. Fourcaud-Trocmé, D. Hansel, C. van Vreeswijk, and N. Brunel, J. Neurosci. **23**, 11628 (2003).
[15]M. Richardson, N. Brunel, and V. Hakim, J. Neurophysiol. **89**, 2538 (2003).
[16]N. Brunel, V. Hakim, and M. Richardson, Phys. Rev. E **67**, 051916 (2003).
[17]R. Llinás, A. A. Grace, and Y. Yarom, Proc. Natl. Acad. Sci. U.S.A. **88**, 897 (1991).
[18]H. G. Rotstein, T. Oppermann, J. A. White, and N. Kopell, J. Comput. Neurosci. **21**, 271 (2006).
[19]J. Csicsvari, H. Hirase, A. Czurko, A. Mamiya, and G. Buzsáki, J. Neurosci. **19**, RC20 (1999).
[20]J. Csicsvari, B. Jamieson, K. D. Wise, and G. Buzsaki, Neuron **37**, 311 (2003).
[21]H. R. Wilson and J. D. Cowan, Biophys. J. **12**, 1 (1972).
[22]L. Glass and M. C. Mackey, *From Clocks to Chaos: The Rhythms of Life* (Princeton University Press, Princeton, NJ, 1999).
[23]B. Lindner and L. Schimansky-Geier, Phys. Rev. Lett. **86**, 2934 (2001).
[24]A. Destexhe, Z. F. Mainen, and T. J. Sejnowski, in *Methods in Neuronal Modeling*, 2nd ed., edited by C. Koch and I. Segev (MIT Press, Cambridge, MA, 1998), pp. 1–25.
[25]L. Lapicque, J. Physiol. Pathol. Gen. **9**, 620 (1907).
[26]B. W. Knight, J. Gen. Physiol. **59**, 734 (1972).
[27]H. C. Tuckwell, *Introduction to Theoretical Neurobiology* (Cambridge University Press, Cambridge, 1988).
[28]M. Abramowitz and I. A. Stegun, *Tables of Mathematical Functions* (Dover, New York, 1970).
[29]B. Hutcheon and Y. Yarom, Trends Neurosci. **23**, 216 (2000).
[30]G. Fuhrmann, H. Markram, and M. Tsodyks, J. Neurophysiol. **88**, 761 (2002).
[31]R. E. Mirollo and S. H. Strogatz, SIAM J. Appl. Math. **50**, 1645 (1990).
[32]W. W. Lytton and T. J. Sejnowski, J. Neurophysiol. **66**, 1059 (1991).
[33]L. F. Abbott and C. van Vreeswijk, Phys. Rev. E **48**, 1483 (1993).
[34]D. Hansel, G. Mato, and C. Meunier, Europhys. Lett. **23**, 367 (1993).
[35]D. Golomb and J. Rinzel, Physica D **72**, 259 (1994).
[36]U. Ernst, K. Pawelzik, and T. Geisel, Phys. Rev. Lett. **74**, 1570 (1995).
[37]W. Gerstner, L. van Hemmen, and J. Cowan, Neural Comput. **8**, 1653 (1996).
[38]C. van Vreeswijk, Phys. Rev. E **54**, 5522 (1996).
[39]W. Gerstner, Neural Comput. **12**, 43 (2000).
[40]C. van Vreeswijk, Phys. Rev. Lett. **84**, 5110 (2000).
[41]D. Hansel and G. Mato, Neural Comput. **15**, 1 (2003).
[42]G. Mato, in *Methods and Models in Neurophysics*, edited by C. Chow, B. Gutkin, D. Hansel, C. Meunier, and J. Dalibard (Elsevier, Amsterdam, 2005).
[43]X.-J. Wang, in *Encyclopedia of Cognitive Science*, edited by L. Nadel (MacMillan, London, 2003), pp. 272–280.
[44]D. A. McCormick and T. Bal, Annu. Rev. Neurosci. **20**, 185 (1997).
[45]G. Buzsaki and A. Draguhn, Science **304**, 1926 (2004).
[46]M. Bartos, I. Vida, and P. Jonas, Nat. Rev. Neurosci. **8**, 45 (2007).
[47]G. Buzsaki, R. Urioste, J. Hetke, and K. Wise, Science **256**, 1025 (1992).
[48]A. Ylinen, A. Bragin, Z. Nadasdy, G. Jando, I. Szabo, and G. Buzsaki, J. Neurosci. **15**, 30 (1995).
[49]E. D. Adrian, Proc. Phys. Soc. **83**, 32 (1934).
[50]C. de Solages, G. Szapiro, N. Brunel, V. Hakim, P. Isope, C. Rousseau, B. Barbour, and C. Léna, "High frequency organization and synchrony of activity in the Purkinje cell layer of the cerebellum," Neuron (submitted).
[51]P. Fries, S. Neuenschwander, A. K. Engel, R. Goebel, and W. Singer, Nat. Neurosci. **4**, 194 (2001).
[52]B. Pesaran, J. S. Pezaris, M. Sahani, P. P. Mitra, and R. A. Andersen, Nat. Neurosci. **5**, 805 (2002).
[53]A. Bragin, G. Jando, Z. Nadasdy, J. Hetke, K. Wise, and G. Buzsáki, J. Neurosci. **15**, 47 (1995).
[54]A. Fisahn, F. G. Pike, E. H. Buhl, and O. Paulsen, Nature (London) **394**, 186 (1998).
[55]E. H. Buhl, G. Tamas, and A. Fisahn, J. Physiol. **513**, 117 (1998).
[56]T. Gloveli, T. Dugladze, S. Saha, H. Monyer, U. Heinemann, R. D. Traub, M. A. Whittington, and E. H. Buhl, J. Physiol. **562**, 131 (2004).
[57]N. Hajos, J. Palhalmi, E. O. Mann, B. Nemeth, O. Paulsen, and T. F. Freund, J. Neurosci. **24**, 9127 (2004).
[58]E. O. Mann, J. M. Suckling, N. Hajos, S. A. Greenfield, and O. Paulsen, Neuron **45**, 105 (2005).
[59]M. Penttonen, A. Kamondi, L. Acsady, and G. Buzsaki, Eur. J. Neurosci. **10**, 718 (1998).
[60]K. MacLeod and G. Laurent, Science **274**, 976 (1996).
[61]B. Bathellier, S. Lagier, P. Faure, and P.-M. Lledo, J. Neurophysiol. **95**, 2678 (2005).
[62]R. D. Traub, D. Schmitz, J. G. R. Jefferys, and A. Draguhn, Neuroscience **92**, 407 (1999).

[63]T. J. Lewis and J. Rinzel, Network **11**, 299 (2000).
[64]A. Draguhn, R. D. Traub, D. Schmitz, and J. G. R. Jefferys, Nature (London) **394**, 189 (1998).
[65]D. Schmitz, S. Schuchmann, A. Fisahn, A. Draguhn, E. H. Buhl, W. Petrasch-Parwez, R. Dermietzel, U. Heinemann, and R. D. Traub, Neuron **31**, 831 (2001).
[66]V. A. Makarov, V. I. Nekorkin, and M. G. Velarde, Phys. Rev. Lett. **86**, 3431 (2001).
[67]A. Roxin, N. Brunel, and D. Hansel, Phys. Rev. Lett. **94**, 238103 (2005).
[68]A. K. Engel, P. Fries, and W. Singer, Nat. Rev. Neurosci. **2**, 704 (2001).